

Abstract:

A versatile graphene/nanofiber aerogel (GNA) with tunable pore structure, wettability and mechanical properties was developed, showing multi-applications in water remediation. The synergistic effect from the two building blocks endows the aerogel with improved mechanical performance, stability in water, and high adsorption capacity for dyes. By modifying the compressed GNA *via* co-deposition of PDA/PEI, the material demonstrates extremely high flux ($> 19000 \text{ L m}^{-2} \text{ h}^{-1} \text{ bar}^{-1}$) and oil rejection ($> 99 \%$) for separation of oil-in-water emulsions. On the other hand, by chemical vapor deposition modification using silane, the GNA exhibits remarkable compressive elasticity and superhydrophobicity and are transformed into a high-performance adsorbent for organic liquids.

Results and discussion

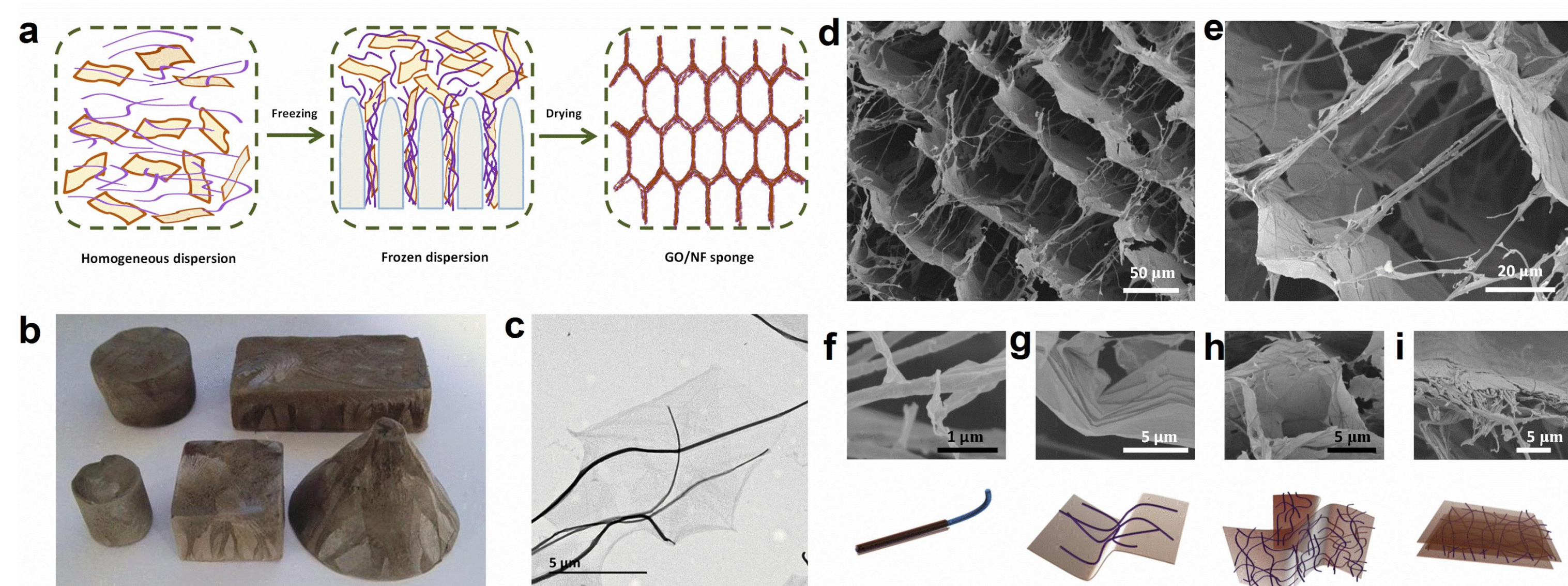


Fig. 1 a) Preparation of GNA *via* a direct freeze-drying procedure. b) Photographs of GNA obtained from different moulds. c) TEM image of GNA deposited on a copper mesh. CA nanofibers of tens of micrometers in length are attached on GO sheets with a large lateral size. d-e) SEM images of GNA showing the interconnected porous structure. f-i) SEM images of GNA showing different sheets/nanofibers combination ways (upper) and the corresponding cartoon models (lower). The GO fraction (f) in all GNA is 0.5.

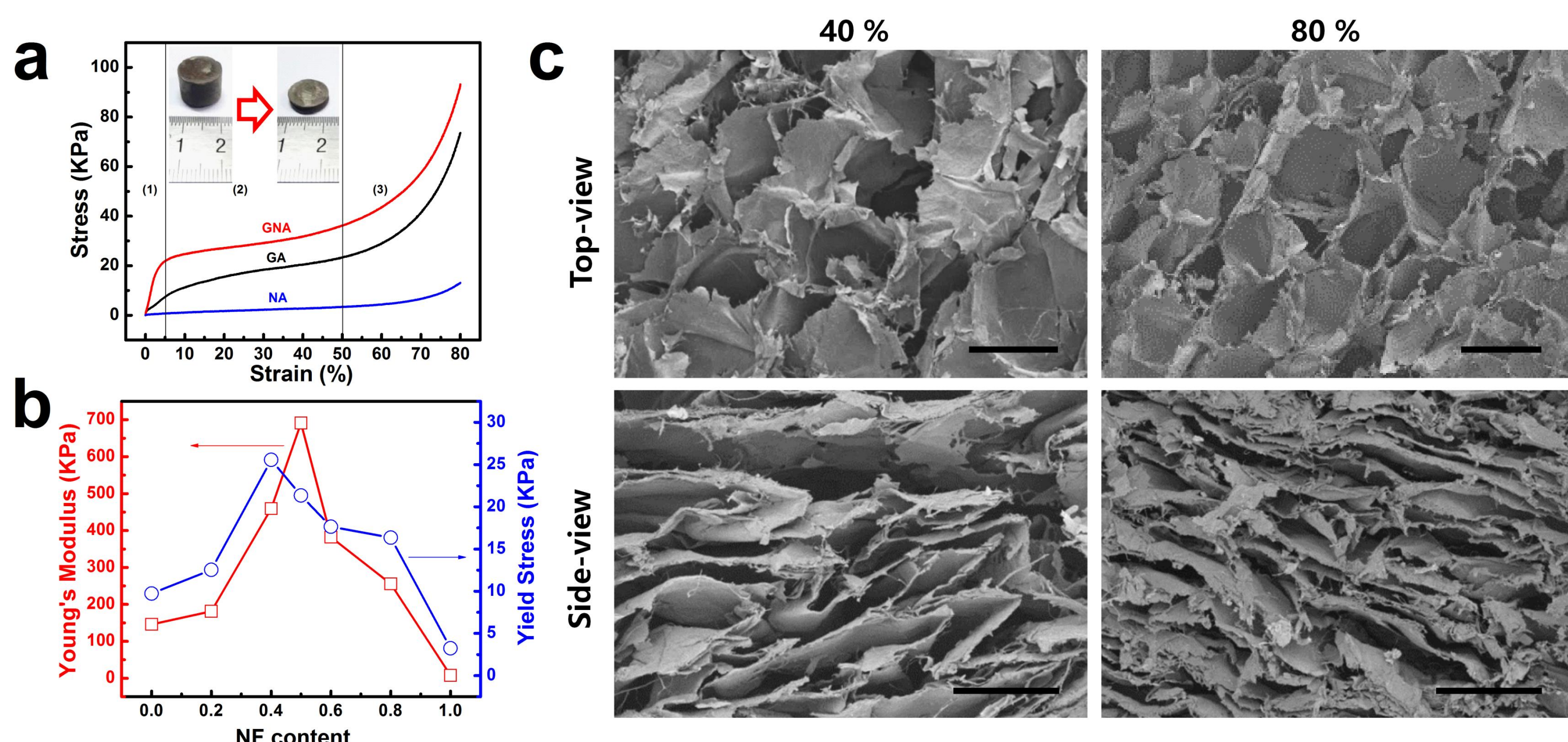


Fig. 2 a) Compression stress-strain curves of GNA ($\rho = 18.4 \text{ mg/cm}^3$, $f = 0.5$), GA and NA. b) Young's modulus and yield stress of GNA as a function of GO fraction. c) Top- and side-view SEM images of GNA compressed to 40% and 80% strains. The inset in (a) shows photographs of GNA before and after compression to 80% strain, and the scale bar in (c) represents 100 μm .

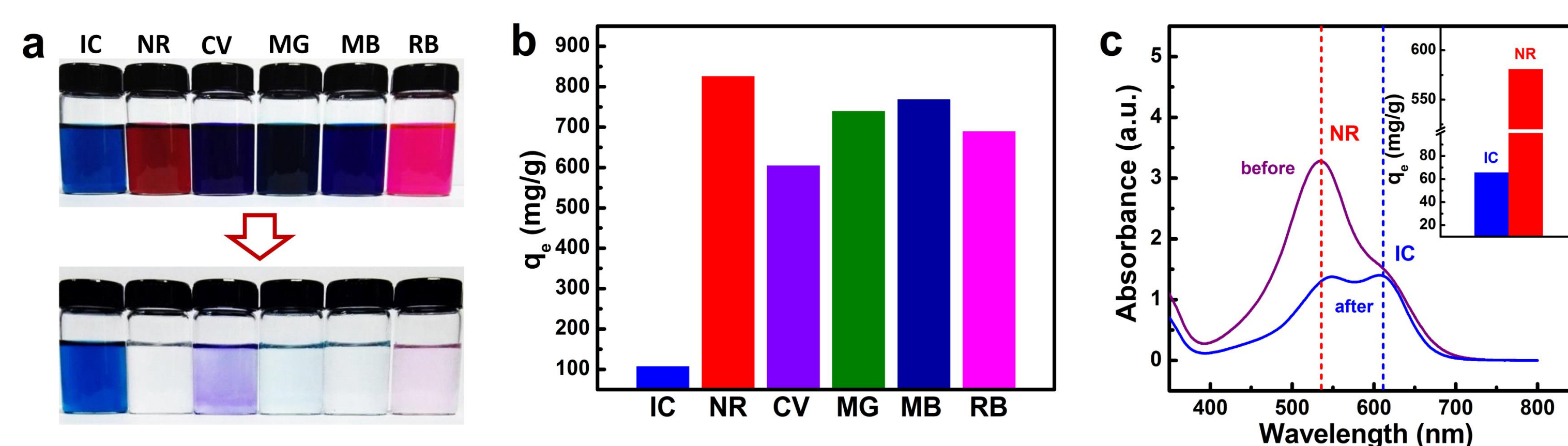


Fig. 3 a) Photographs of various dye solutions (100 mg/L) before and after adsorption using GNA ($\rho = 18.3 \text{ mg/cm}^3$, $f = 0.625$). b) q_e of GNA for different dyes (500 mg/L). c) UV-Vis spectra of NR/IC binary dye solution before and after adsorption. Inset in (c) shows q_e of IC and NR, respectively.

Conclusions

The pore structure, wettability and mechanical properties of GNA are tunable to multi-applications in water remediation. The introduction of nanofibers brings improved mechanical performance, stability in water, and high adsorption capacity for cationic dyes. After compression at high strain and hydrophilic modification, the aerogel can separate oil-in-water emulsions with high flux and oil rejection. The modification *via* silane provides the aerogel with superhydrophobicity, compressive elasticity and high adsorption capacity for organic liquids. Thus GNA exhibits great application potential in multiple fields of water treatment.

Acknowledgement

This work was supported by the National Natural Science Foundation of Zhejiang Province (Grant No. R14E030003), the National Natural Science Foundation of China (Grant No. 51573157, 51333004, and 51373149).

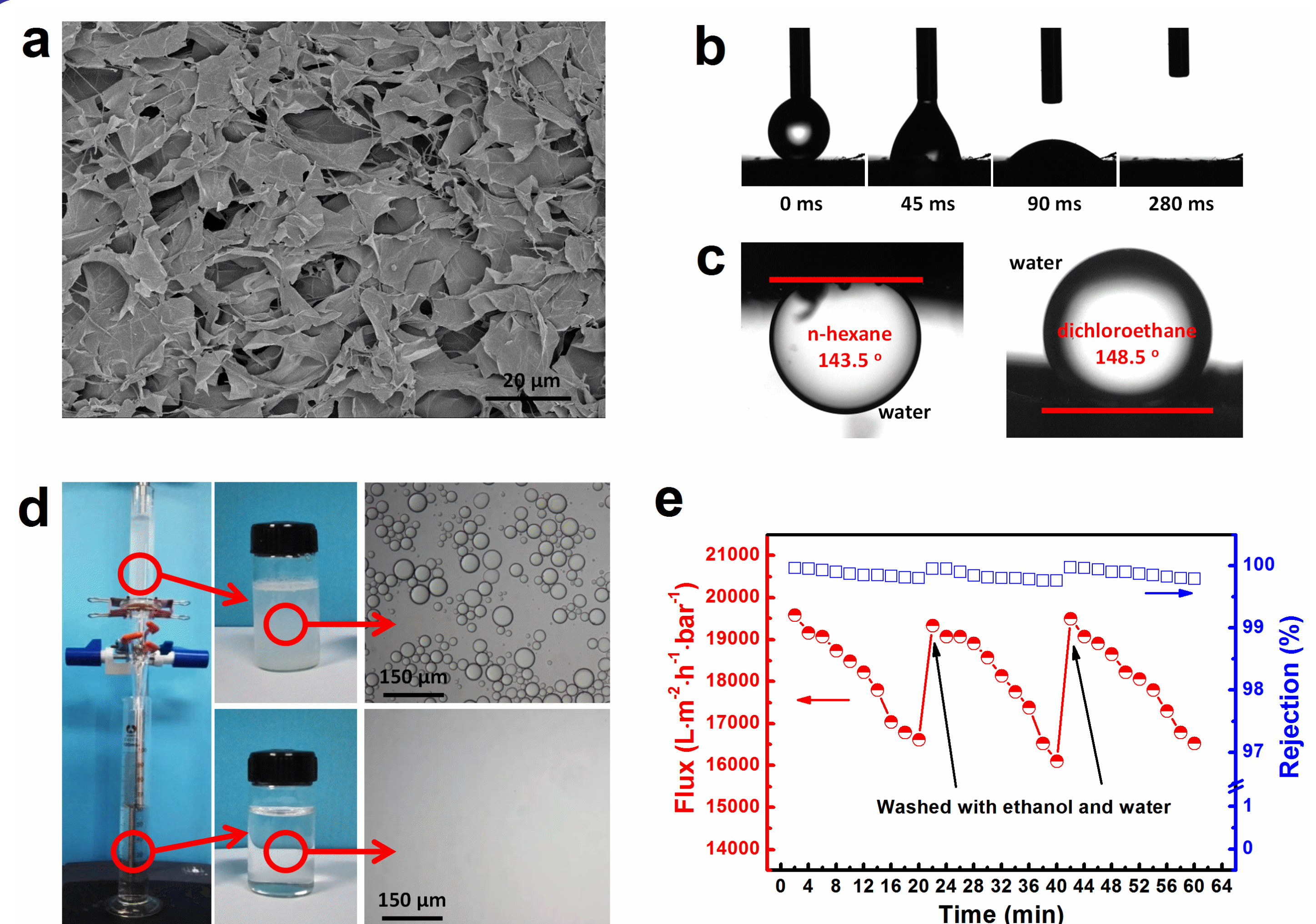


Fig. 4 a) SEM image of GNA-1 ($f = 0.5$, $\rho = 18.4 \text{ mg/cm}^3$) with pore size of 5-10 μm . b) Fast permeation of water on the surface of GNA-1. c) Underwater contact angle of *n*-hexane and 1,2-dichloroethane on GNA-1. d) The gravity-driven separation of oil-in-water emulsions using GNA-1 and microscopic images of emulsions before and after separation. e) Flux and rejection of *n*-hexane-in-water emulsion.

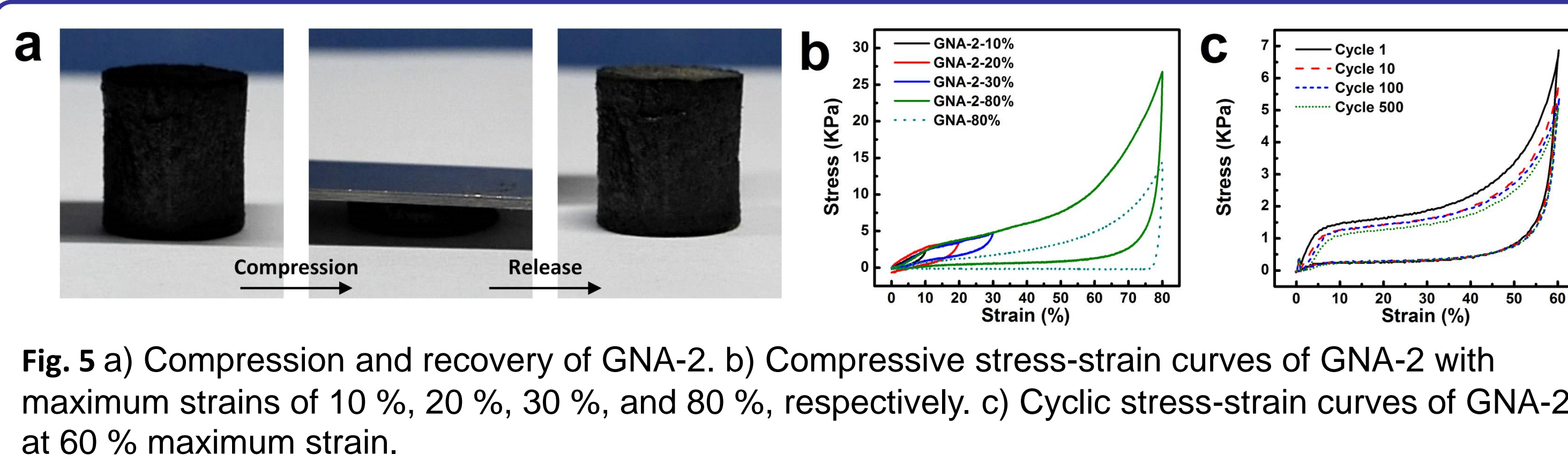


Fig. 5 a) Compression and recovery of GNA-2. b) Compressive stress-strain curves of GNA-2 with maximum strains of 10%, 20%, 30%, and 80%, respectively. c) Cyclic stress-strain curves of GNA-2 at 60% maximum strain.

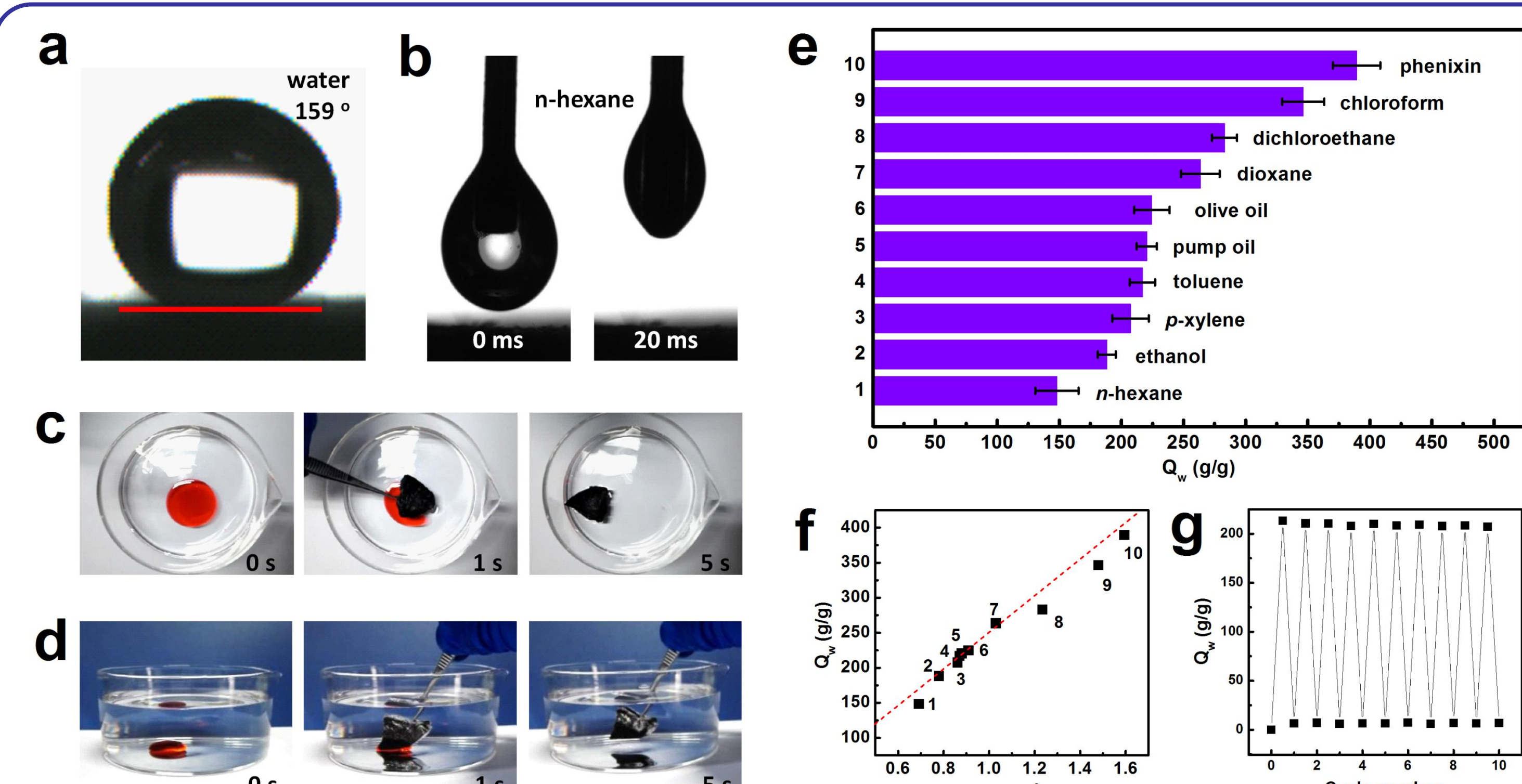


Fig. 6 a) Superhydrophobic surface of GNA-2. b) Fast permeation of *n*-hexane on the surface of GNA-2. c-d) Absorption process of toluene (stained with OR) spreading on water and 1,2-dichloroethane by GNA-2. e) Q_w of GNA-2 for various oils and organic solvents. f) Q_w as a function of ρ for various organic liquid identified by numbers. g) Recyclability of GNA-2 for the adsorption of toluene under 10 cycles.

References

- Si, Y.; Fu, Q.; Wang, X.; Zhu, J.; Yu, J.; Sun, G.; Ding, B., *Acs Nano* **2015**, *9* (4), 3791-3799.
- Yang, H. C.; Pi, J. K.; Liao, K. J.; Huang, H.; Xu, Z. K., *ACS Appl. Mater. Interfaces* **2014**, *6* (15), 12566-12572.
- Sun, H.; Xu, Z.; Gao, C., *Adv. Mater.* **2013**, *25* (18), 2554-2560.
- Li, F.; Du, M.; Zheng, Q., *Acs Nano* **2016**, *10* (2), 2910-2921.